BMC Infectious Diseases

RESEARCH

Open Access

Malaria exposure remodels the plasma proteome of Ghanaian children

Aisha M. Mohammed[1,2†], Charles Ochieng' Olwal[1,2†], Andrea Fossati[3,4,5†], Nancy K. Nyakoe[1,2], Jacqueline M. Fabius[3,4,5], Martin Gordon[4,5], Benjamin J. Polacco[4,5], Danielle L. Swaney[3,4,5*], Gordon A. Awandare[1,2*], Nevan J. Krogan[3,4,5*], Mehdi Bouhaddou[6,7,8*] and Yaw Bediako[1,9*]

Abstract

Background Malaria, caused by *Plasmodium falciparum*, remains a major public health burden causing ~ 200 million deaths annually, especially among children. Although the lack of an effective vaccine has hindered malaria elimination, studies have reported on individuals acquiring natural immunity to malaria in the context of high malaria exposure. However, the immune correlates of protection in these people who acquire natural immunity against malaria are poorly understood.

Methods Symptomatic children residing in high and low malaria transmission areas of Ghana were enrolled into the study and followed for 3 weeks from the day of malaria confirmation. The plasma proteome of these children was profiled using a mass spectrometry-based approach and putative protein-based biomarkers and predictors of immune tolerance to malaria were identified.

Results We identified several differentially abundant proteins in children living in high malaria transmission areas relative to children in low transmission areas. Differentially abundant proteins were enriched in immune response processes, including complement cascade activities and elevated platelet activation. We found IGKV3D-20 protein to be strongly associated with high malaria exposure.

Conclusions Our findings confirm earlier reports and identify putative signature proteins implicated in immune tolerance to malaria. Further large-scale and more mechanistic studies will be needed to reveal the key components of the identified pathways that could explain naturally acquired immunity to malaria and possibly be exploited to develop novel therapeutics against P. falciparum.

†Aisha M. Mohammed, Charles Ochieng' Olwal and Andrea Fossati these authors contributed equally.

*Correspondence:
Danielle L. Swaney
danielle.swaney@ucsf.edu
Gordon A. Awandare
gawandare@ug.edu.gh
Nevan J. Krogan
nevan.krogan@ucsf.edu
Mehdi Bouhaddou
bouhaddou@ucla.edu
Yaw Bediako
ybediako@ug.edu.gh
Full list of author information is available at the end of the article

Keywords Malaria immunity, Plasma proteomics, Antibodies, IGKV3D-20, Complement cascade, C1QA, Malaria transmission

Background

Malaria, caused by *Plasmodium falciparum*, is a major public health burden, particularly in sub-Saharan Africa [1], with high mortality rates for children under 5 years of age and pregnant women [2]. According to the World Health Organization (WHO), malaria cases rose from 244 million in 2021 to 249 million in 2022, with the majority occurring in WHO African region [3]. Several factors, including antimalarial drug resistance, insecticide-resistant mosquito vectors and the absence of an effective vaccine, contribute to the persistence of malaria. Thus, better counterstrategies are needed to control and/or eliminate malaria [1].

Individuals in malaria-endemic areas develop immunity to malaria after multiple exposures over time [4], and require continuous malaria parasite exposure to remain immune against malaria [5]. Due to frequent exposure to malaria parasites, individuals in high malaria transmission (HMT) areas tend to develop natural immunity against malaria and are more tolerant to malaria compared to those living in lower malaria transmission (LMT) areas [6]. However, the correlates of protection against malaria for individuals in HMT remain poorly understood. If known, these could accelerate the design of effective vaccines and therapies against malaria.

A number of prior studies have demonstrated that naturally acquired immunity (NAI) to malaria involves immune modifications induced by multiple infections, manifesting in unique cytokine and cellular immune signatures that differentiate between individuals of differing prior exposure to malaria [5, 7]. An earlier study compared the immune signatures of malaria-naive Europeans to Africans with lifelong exposure. These studies found that Africans were more capable of controlling *P. falciparum* parasitemia than their European counterparts [8]. Another study also carried out a study on Ghanaian children with malaria to identify parasite antigens associated with clinical immunity and reported 15 antigens that have shown a strong correlation with immune status [9]. At the level of the host proteome, a previous study has characterized the altered proteome of the frontal lobe of cerebral malaria patients, identifying signatures of disease pathophysiology and demonstrating how the aftermath of infection results in the production and secretion of antibodies into the bloodstream [10]. However, the definitive mechanism of naturally acquired immunity to malaria remains unclear.

For this study, we hypothesized that relative to children in LMT areas, children in HMT areas differentially express certain proteins in their bloodstream that protect against malaria. This hypothesis was motivated by previous observations that naturally acquired immunity against malaria results from multiple malaria episodes [5, 6, 11]. The hypothesis is further motivated by a previous observation that children more frequently exposed to malaria acquire natural immunity against the disease faster than those who are less exposed [6]. To test this hypothesis, we harnessed an unbiased global quantitative mass spectrometry (MS) based proteomic analysis of plasma samples from children (5–14 years old) in LMT and HMT areas collected across three-time points, that is, day 0 (parasite detected and therapy initiated), day 7 (recovery) and day 21 (post-recovery). We highlight several immune-related proteins and pathways differentially regulated in individuals from HMT across the three time-points relative to those from LMT areas.

Materials and methods

Sample size determination and ethical clearance

This study was part of a larger longitudinal study. For this study, 60 patients were randomly selected, inclusion criteria being that the patients must have completed the 3 visits and blood samples collected, should have been diagnosed with malaria on the first visit, and not have any hemoglobinopathies. Ethical clearance was obtained from Noguchi Memorial Institute for Medical Research Institutional Review Board (NMIMR) (Approval number: NMIMR-IRB CPN 008/17–18).

Study sites

The study was conducted in two ecologically different regions of Ghana: the Greater Accra region (Ledzokuku Krowor Municipal Assembly (LEKMA) hospital) and Bono East region (Kintampo Health Research Center (KHRC)). The Bono East region, where the Kintampo district is located has forest-savannah vegetation and experiences a double maxima rainfall regime. This drives agricultural activity making it a high breeding site for mosquitoes and malaria infections [12]. The malaria transmission here is high all year round, with entomological inoculation rate (EIR) greater than 250 infective bites/person/year [13]. Meanwhile, the greater Accra region experiences a tropical rainfall pattern, with fewer agricultural activities. It is an urban area where opportunities for

mosquito bites and malaria infection are quite low. More so, malaria transmission is generally low in Accra with EIR of 50 infective bites/person/year but has a peak transmission season, which is the early rainy season [13].

Sample collection and malaria case definition

Children aged between 5 and 14 years old presenting to the hospital with fever and further diagnosed with malaria were voluntarily enrolled in the study after obtaining written informed consent from their parents or legal guardians. Blood samples were collected from both sites simultaneously, within the same time frame (October 2017 to January 2019). Acute *P. falciparum* malaria infection was confirmed when the child had a fever, a positive result for malaria rapid diagnostic test (RDT) and further confirmation by microscopy. Parasite density was determined by the number of parasites/200 white blood cells (WBCs) * total number of WBCs [14]. For the age range of our study: 5 – 14 years, a parasite density of 1000 parasites/ul or more was used to define acute malaria [13]. The study participants were treated with either Artemether/lumefantrine or Artesunate amodiaquine. 10 ml of whole blood samples was collected by venipuncture into BD-citrate EDTA vacutainer tubes at three-time points (i.e., day 0, Day 7, and Day 21). The samples were transported to the laboratory in cold chain where the parasite density was determined using a microscope. Whole blood was centrifuged with Eppendorf centrifuge 5804R, with a radius of 15.9 cm. The spinning conditions were set to 2500 rpm (1,118*g) with no breaks for 15 min and the plasma was carefully collected into cryotubes and stored at -80 °C until use. For this study, 60 plasma samples were randomly selected, 30 from low malaria transmission (LMT) and 30 from high malaria transmission (HMT) site. All the selected samples had samples from all the 3 visits.

Protein digestion and peptide preparation

Plasma protein was digested into peptides in three main steps using the iST-BCT sample preparation kit (PreOmics GmbH, 82,152 Martinsried, Germany) following the manufacturer's protocol with minor modifications. The three main steps involved lysis, reduction and alkylation of the samples at 95 °C for 10 min and digestion of total plasma proteins at 37 °C for 60 min using LysC and trypsin. Peptides desalting was done as per the manufacturer's instruction in two washing steps before final elution. Peptides were dried by centrifugation at 45 °C, 25 inches mercury (634.99 mmHg) for 180 min using the Labonco Speed-Vac.

To perform reverse phase basic fractionation, samples were acidified to a final concentration of 0.1% TFA. C18 spin columns (Nest group) were activated with 1 column volume of acetonitrile (ACN) and equilibrated with two column volumes of 0.1% TFA. Peptides were bound to the column and washed twice with 0.1% TFA. For elution, solutions of increasing concentration of ACN in 0.1% triethylamine from 2.5% to 20% were used. After the last elution the column was washed twice with 1 column volume of 50% ACN. Fractions were dried under vacuum and resuspended in 15 µl Buffer A (0.1% FA in MS grade H_20) and approximately 500 ng were subjected to proteomics analysis as previously described by [15]. However, no peptides were detected in three patient samples; hence, were not included in the analyses.

Spectral library generation through DDA PASEF acquisition

Peptides were passed through a manually packed 15 cm long column packed with 1.7 µm BEH beads (Waters) packed with Silica PicoTip Emitter (ID 75 µm) (New Objective, Woburn, USA) at a flow rate of 400 nl/minute. The separated peptides were eluted with buffer B (80% acetonitrile and 0.1% formic acid in HPLC-H2O) in a linear gradient from 2 to 32% in buffer A (0.1% formic acid in HPLC-H2O) for 120 min. The peptides were injected into the timsTOF Pro using a CaptiveSpray source (Bruker) with an endplate offset of 500 V, a dry bulb temperature of 200 °C and a capillary voltage fixed at 1.6 kV. The positive ion mode was used in the operation of the mass spectrometer. Data Dependent Acquisition (DDA) was performed by running the timsTOF Pro (Bruker) in PASEF mode with Compass Hyster v5.1 and TOF control v6.2. The mass range was set at 100–1700 m/z, with 10 PASEF scans between 0.6 Vs/cm2 and 1.6 Vs/cm2. 2 ms and 100 ms were set for the accumulation and ramp times, respectively. Fragmentation was adjusted to occur at 20,000 arbitrary units (a.u.) and then the peptides were fragmented using collision-induced dissociation (CID) with a spread between 20 and 59 eV [15].

DIA PASEF acquisition

Data Independent Acquisition (DIA) for each sample was performed with HPLC–MS, just as it was performed for the DDA using a 45-min chromatographic gradient. The separation and column were set at 400 nl/minute and 500 nl/minute, respectively, to perform separation and washing. The same MS1 regions, PASEF parameters, and fragmentation parameters as described in the DDA-PASEF acquisition were also used in the DIA-PASEF acquisition, and 12 DIA-PASEF scans per cycle were performed [6].

Mass spectrometry data analysis

Spectral library generation

The sample-specific library for DDA was generated using the FragPipe (version 15) computing platform with

the components MSFragger (version 3.2), Philosopher (version 3.4.13), and EasyPQP (version 0.1.9) [16]. The MSFragger search engine was used to identify the peptides from the tandem mass spectra (MS/MS) using the raw material.d files as inputs. The protein sequences of Homo sapiens with UniProt ID UP000005640 and Plasmodium falciparum with ID UP000001450 were downloaded from the UniProt database (https://www.uniprot.org/) on July 15, 2021. Reverse sequences were used as decoys for false discovery rate (FDR) estimation. For the MSFragger analysis, the speclib working pipeline was set [16]. The precursor and initial fragment mass tolerances were set to 20 ppm, spectrum deisotopicization, mass calibration, and parameter optimization were all enabled. The enzyme specificity was adjusted to strictrypsin to allow cleavage before proline. Missed trypsin cleavages were set to 2 and the isotopic error was set to 0/1/2. The peptide length was adjusted to 7 to 50 and their masses to a range of 500 to 5000 Da. The oxidation of methionine, the acetylation of protein N-termini, the loss of water at the N-terminal glutamic acid and pyroglutamate Da at the N-terminal glutamine were defined as variable modifications. The carbamidomethylation of cysteine was defined as a fixed modification. The maximum number of variable modifications per peptide was set to 3. Peptide and protein-level FDR were fixed to 1%. The filtered PSM.tsv files and uncalibrated MGF files created by MSFragger from the raw. d files were used as inputs to EasyPQP to generate unified spectral libraries.

DIA data analysis

DIA-NN was used for dia-PASEF data processing, using the one generated by easyPQP as the spectra library. The maximum mass accuracy tolerance has been set to 10 ppm for MS1 and MS2 spectra. The protein inference for DIA-NN was disabled and the protein groups from ProteinProphet were used. The quantification mode was set to Robust LC (high precision) and other settings were set to the default values. Finally, the DIA-NNs output was filtered at precursor Q < 1% and global protein Q < 1%.

Across all our samples, we detected a total of exactly 900 proteins. We calculated the percent missingness in each sample for each protein and annotated each as greater than or less than 50% missingness. Only 28/900 (3.1%) of these proteins never achieved less than 50% missingness in any patients, at any time point.

Data processing and analysis

Analysis of changes in protein abundance between patient cohorts was performed using outputs from DIA-NN and processed using artMS as described previously [17]. In brief, changes in the protein abundance were quantified using artMS version 1.18.0 as a wrapper around MSstats version 4.8.7, via artMS::artmsQuantification function using default settings. In MSstats, normalization is performed by median equalization, no imputation of missing values, and median smoothing to combine intensities for multiple peptide ions or fragments into a single intensity per protein. Finally, we analysed the statistical differences in intensity between patient cohorts. Unless otherwise indicated, defaults for MSstats for adjusted p-values were used even in cases of n = 2. By default, MSstats utilises the Student's t-test for p-value calculation and the Benjamini–Hochberg method for estimating FDR to adjust p-values. To correct for batch effects in our abundance proteomics data, we employed the `removeBatchEffects` function from the `LIMMA` package (version 3.54.2). Briefly, the function fits a linear model to data including terms for batch and 'interesting' explanatory variables (site + timepoint), estimates the batch coefficient and subtracts this from the original matrix, returning a residual matrix free of batch effects.

Pearson's r correlations were calculated by correlating the intensities of each protein quantity between pairs of patients after cross-run normalization and summarization of peptides to proteins. The fraction overlap was calculated as the fraction of total detected proteins, between each pair of patients, that was detected in both patients.

Data analysis and code availability

Bioinformatics analysis and data visualization of the proteomics data were performed using various packages anchored in R version 4.4.1 (R Development Core Team, Vienna, Austria) and RStudio version 2024.09.0 + 375. No new codes were developed in this study.

Results

Patient characteristics and study design

In this study, we set out to identify a proteomic signature characteristic of naturally acquired malaria tolerance as seen in HMT areas. To achieve this, we used quantitative liquid chromatography mass spectrometry (LC–MS)-based proteomic analysis to identify differences in the plasma proteome between children from HMT ($n = 30$) and LMT ($n = 30$) areas in Ghana. The map of Ghana (Fig. 1A) shows the malaria prevalence across all the regions of Ghana [18], highlighting the study sites. Bono East region (red dot, HMT) and Greater Accra (Green dot, LMT). All the children had at least 1 recorded malaria episode per year, which includes the current episode at the time of recruitment into the study, with children from HMT site recording higher malaria episodes per year (Fig. 1B). Similarly, higher parasite densities were also recorded in HMT (Mean HMT = 92,820.5 PD/μL) relative to LMT (Mean LMT Mean = 39,284.6 PD/μL) (Fig. 1C). Inversely, a lower average body temperature at

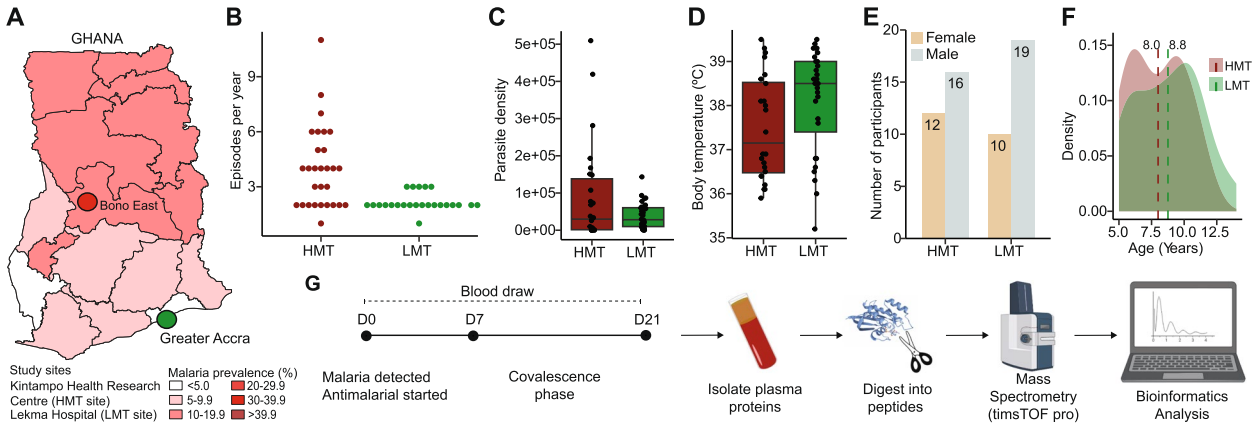

Fig. 1 Study participants overview and mass spectrometry experimental workflow. **A** The study was conducted in the high (red) and low (green) malaria transmission areas in Ghana. The map is adapted from Ghana Demographic and Health Survey, 2022 [18]. **B** Average malaria episodes recorded per year and (**C**) average parasite densities of the participants were recorded. **D** Recorded body temperature of participants at D0.(**E**) A bar plot showing gender distribution of the study participants. **F** The age distribution of the study participants between HMT and LMT sites. **G** A pipeline of the workflow employed from sample collection through to data analysis. Blood samples were collected from children with acute malaria at days 0, 7, and 21. Plasma was separated from the blood, and plasma proteins were digested into peptides prior to LC–MS and bioinformatics analyses. Additional file 1 provides all the data used to generate figures B-F

time of diagnosis was recorded in HMT (37.5 °C) compared to LMT (38.1 °C) (Fig. 1D), suggesting reduced symptomology in the HMT cohort. A positive correlation between average body temperature and parasite density was observed, with LMT showing a higher average body temperature with lower parasite density than HMT (Figure S1). Both males and females were represented at both sites, with slightly more males (Fig. 1E). The participants were aged between 5 to 14 years and the age distributions were comparable between the two groups (Fig. 1F). In this longitudinal study, plasma was separated from patient blood drawn on day 0 (D0), 7 (D7) and 21 (D21), corresponding to malaria diagnosis and initiation of therapy, recovery and post-recovery, respectively. Plasma proteins were digested into peptides prior to LC–MS/MS analysis using a Bruker timsTOF Pro mass spectrometer and downstream bioinformatics analyses (Fig. 1G). Taken together, these observations suggest that children in the HMT site experience a larger number of malaria episodes, and present with lower body temperatures, despite higher parasitemia compared to children living in the LMT area.

Plasma proteome profiling of children from HMT and LMT areas

Following data independent acquisition MS (DIA-MS) analysis, we detected over 500 proteins in both groups of children (Fig. 2A), which is consistent with the range of proteins detected in plasma samples previously [19, 20]. Interestingly, while protein counts were constant over time for the HMT group, they increased in the LMT group at D7 and D21, suggesting a stronger response to treatment in the LMT group. Since our samples were processed and analysed by MS in two batches, we first decided to check whether a batch effect was present. A principal component analysis (PCA) of the protein intensities across the patients revealed a considerable batch effect (Fig. 2B). We performed an in silico batch correction procedure which eliminated the inter- and intra-patient variations (Fig. 2C and D). In addition, the fraction overlap in detected proteins per site, compared within and between batches, showed a higher overlap within batches (Fig. 2E). These observations indicated that the underlying biology is preserved between the two batches.

A principal component analysis of patients based on time-point (day) and site showed minimal segregation, 16% for PC1 and 8% for PC2 (Fig. 2F), suggesting that the composition of the plasma proteome does not differ substantially between the two groups. However, an averaged PCA of the protein intensities shows a complete separation of the protein intensities. PC1 shows 34% separation of the protein intensities between D0 (left) and D7; D21 (right) while PC2 shows 27% separation between the LMT (bottom) and HMT (top) (Fig. 2G). Altogether, these results suggest that while the composition of the immune response may not differ much between HMT and LMT, there is a measurable difference in the abundance of plasma proteins between exposure groups, which is apparent at D0, before treatment. The increased abundance of plasma proteins in LMT is possibly indicative of a stronger (more inflammatory) immune response to the infection.

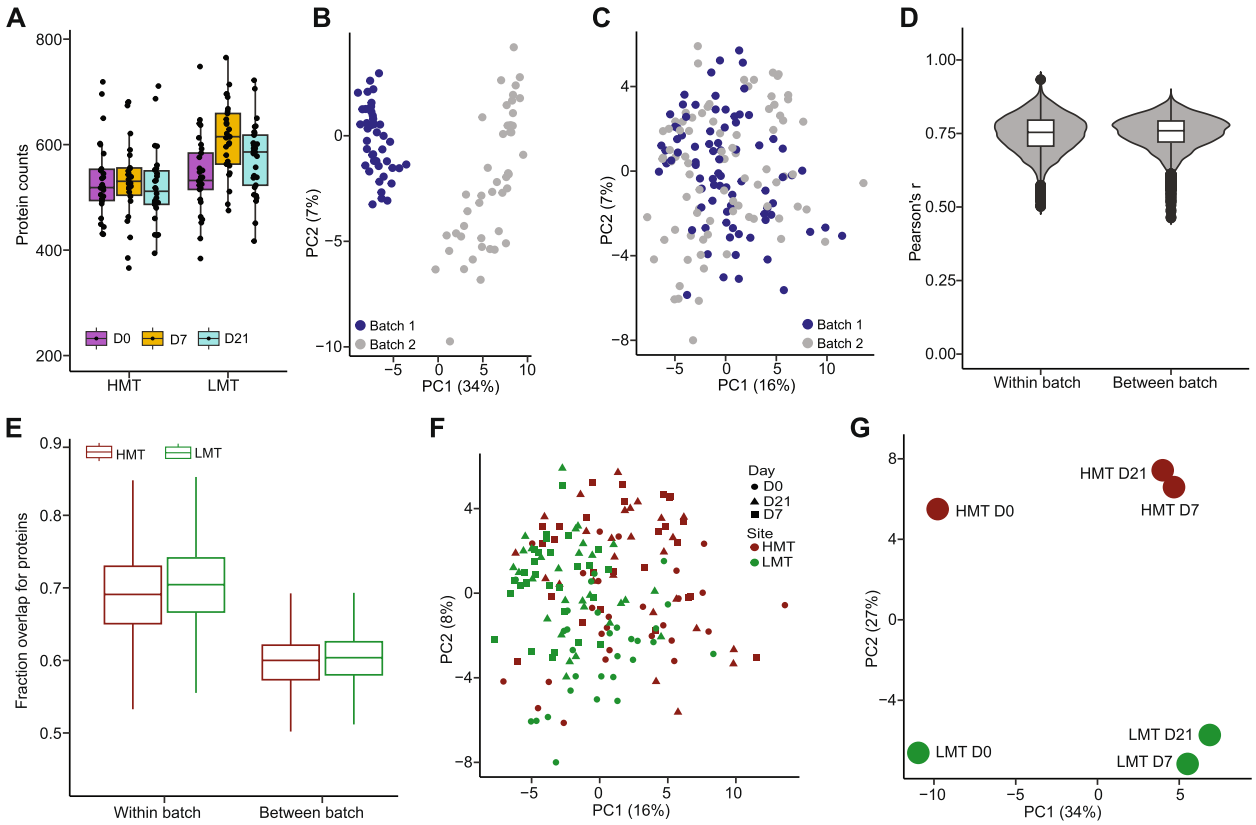

Fig. 2 Plasma proteome reflects differences between malaria transmission zones. **A** The number of proteins detected within each site, per time point, per patient. **B** PCA of protein intensities across two batches before batch correction. (**C**) PCA of protein intensities across the two batches after batch correction **D** The correlation (Pearson's r) of identified protein abundance within and between experimental batches. **E** The fractional overlap of detected proteins within and between experimental batches. For all boxplots, the middle line represents the median, the box limits represent the interquartile range (IQR), and the whiskers mark 1.5-fold increase or decrease beyond the IQR. (**F**) PCA showing the clustering of patients based on day and site. **G** Principal components analysis (PCA) of protein intensities averaged per site and time point. HMT and LMT are depicted in red and green, respectively. All the post-batch correction data used to generate figures A-F are presented in additional file 2. Additional file 3 provided the intensity values before batch correction

Differentially abundant proteins are enriched in immune response processes

In order to identify the changes occurring in the plasma proteome in the course of infection through recovery, we sought to identify proteins that were differentially abundant between different malaria transmission zones (i.e., HMT versus LMT). To achieve this, we statistically quantified changes in plasma protein abundance of patients between LMT and HMT zones. We used absolute value $\log_2$ fold change (FC) > 0.5 and adjusted p-value < 0.05 as cutoffs. Based on this criterion, we identified 8, 47, and 26 differentially abundant proteins (DAPs) in plasma collected on D0, D7, and D21, respectively, 97.5% of which were upregulated in LMT (Fig. 3A). Preliminary gene set overrepresentation analysis (GSOA) on DAPs identified enrichment in platelet elevation, complement, and coagulation cascade pathways (Fig. 3B). We categorized the DAPs into groups depending on the log2FC threshold. We had DAPs at each time-point at log2FC between 0.5 and 1, and also at log2FC greater than 1 (Fig. 3C). Interestingly, we noticed the strongest differences at D7, potentially reflecting a response to antimalarial therapy and/or parasite clearance. Altogether, these analyses suggested that certain proteins are differentially abundant in children from LMT compared to those from HMT. This could account for the differences in the tolerance against malaria seen between the two populations.

Plasma proteome dynamics reveal time- and location-dependent response pathways

Next, we compared the plasma proteome dynamics across the 21-day time course between LMT and HMT zones. We performed hierarchical clustering on the differential expression log2 fold changes between the LMT and HMT zones across time (Fig. 4A). We next used k-means clustering to segregate the proteins into 4 clusters (Fig. 4B-C). We noted the proteins in cluster 1 were downregulated in LMT relative to HMT at D0 followed

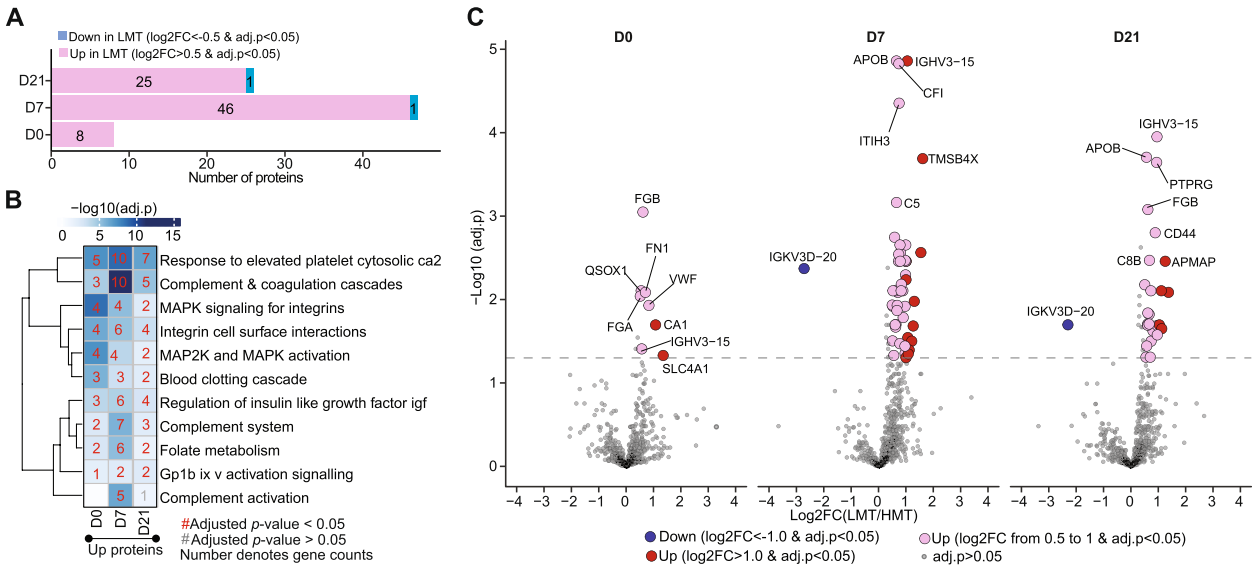

Fig. 3 Plasma proteome differences are enriched in immune response processes. **A** The number of differentially-abundant proteins (DAPs) at the various time-point between LMT and HMT. Upregulated proteins indicates higher abundance in LMT relative to HMT, and vice-versa. A $|\log_2$ fold change (FC)$|>0.5$ and adjusted *p*-value <0.05 were used as cutoffs. The DAPs were determined based on the data provided in additional file 4. **B** Gene set overrepresentation analysis of DAPs using Canonical Pathways subset from the Molecular Signatures Database (https://www.gsea-msigdb.org/gsea/msigdb). A complete enrichment table is provided as additional file 5. **C** Volcano plot showing the expression of the DAPs in LMT versus HMT. Colours represent DAPs at two different log2FC thresholds

by a steady equilibration towards no change following treatment at D7 and D21. Proteins in cluster 1 were enriched in carbohydrate metabolism, inflammatory responses, and complement responses. Proteins in cluster 2 possessed a highly dynamic trajectory: upregulated in LMT relative to HMT at D0, then downregulated at D7, followed by a return to upregulated at D21. Proteins in cluster 2 were enriched in notch signaling, proteosome, cell cycle progression, stress, and apoptosis pathways. Proteins in cluster 3 constituted the largest group and were largely unchanged over time. Proteins in cluster 4 possessed the opposite trend as cluster 1, upregulated in LMT relative to HMT at all time points, depicting a further increase at D7 and D21. Proteins in cluster 4 were enriched in stress responses, extracellular matrix, integrins, MAPK pathway, and growth factor signaling. Interestingly, clusters 2 and 4 both depicted upregulation in LMT relative to HMT at D0 and possess several pathway-level similarities related to stress responses and growth factor-related signaling. The relevance of these pathways in contributing to, or serving as biomarkers for, malaria tolerance in the HMT group requires further investigation by future studies.

Complement proteins and antibody IGKV3D-20 represent baseline differences between LMT and HMT zones

As described above, we identified DAPs to be enriched in platelet activity, complement signaling, and antibody responses. Hence, we sought to identify the specific platelet, complement, or antibody proteins responsible for this effect. We curated a list of known platelets, complement system, and antibody/immunoglobulin proteins from HUGO Gene Nomenclature Committee (HGNC) database and extracted these proteins from our dataset. We analysed trends of platelet (Fig. 5A), complement (Fig. 5B), and antibody (Fig. 5C) protein log2 fold changes in expression between LMT and HMT at each time point. Altogether, we noticed that the expression of all these proteins peaked on D7 and dropped slightly on D21, suggesting that the correlates of malaria tolerance were triggered by malaria infection and increased during recovery but waned post-recovery. A detailed investigation of each protein expression (Fig. 5D-F) indicated that, a group of complement proteins (C8G, C5, C4B, C8B, C3, C2, C8A, C1S, and C6) were downregulated in HMT but upregulated in LMT across the time points. However, we observed that the antibody IGKV3D-20 was highly expressed in HMT in D7 and D21 of HMT but lowly expressed in LMT across all time points (Fig. 5F). Further assessment of C1QA and IGKV3D-20 protein intensities across sites and time revealed that, although not statistically significant, the intensity of C1QA was higher in LMT at all time-points (Fig. 5G). However, the antibody, IGKV3D-20, depicted higher intensity in HMT site children, corresponding to the observation made in Fig. 5F. Taken together, these observations suggest that

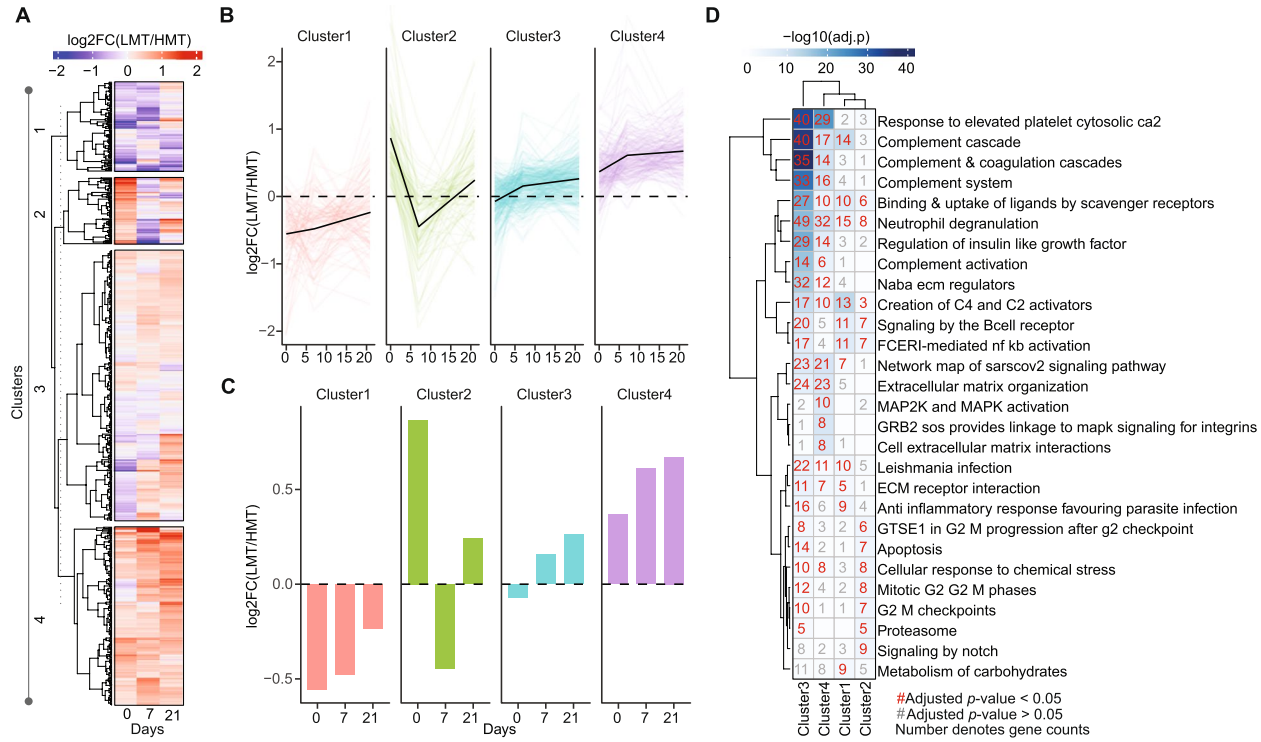

Fig. 4 Plasma proteome dynamics reveal time-dependent and time-independent immune response pathways. **A** Hierarchical and k-means clustering of log2FC to separate proteins into four clusters based on their dynamical regulation over time between LMT and HMT. **B** Line plot of each protein differential abundance (LMT/HMT) over time (coloured lines). Black lines indicate the average. **C** Bar plot of the average differential protein abundance at each time point, in each cluster. **D** GSOA of the top enriched pathway per cluster. A complete enrichment table is provided in additional file 6

the complement system and IGKV3D-20 play an important role in promoting malaria tolerance among individuals frequently exposed to *P. falciparum*.

Discussion

Malaria remains a major public health burden. Although individuals from HMT areas acquire natural immunity against malaria, the molecular mechanisms underlying their tolerance against this disease remain poorly characterized. Here, we used a quantitative LC–MS/MS proteomics approach to profile the plasma proteome of children with acute malaria from LMT and HMT in Ghana. We identified putative correlates and markers of tolerance against malaria, which differentiate individuals from LMT and those in HMT areas in Ghana and could be mechanistic mediators of naturally acquired immunity to malaria.

Analysis of the variation in the expression of protein abundances between LMT and HMT revealed several DAPs. Pathway enrichment analysis of the DAPs indicated that complement and coagulation cascades were enriched. The complement pathway has been linked to malaria immune response, known to be activated by antimalarial immunoglobulin antibodies [21] and has been reported in earlier studies to be severely depleted in cases of severe malaria in children [22, 23]. In addition, a major contributor of the elevated protein response in LMT at D7 is likely driven by the activation of immune response pathways and accumulation of immune cells in response to treatment. Specifically, we observed an elevated platelet response in the LMT group at D7 and D21 (Fig. 5A, 5D). Platelets have been associated with parasite clearance in malaria pathogenesis [reviewed in 17] and are known to increase in the blood as the infection is cleared [24]. These innate immune cells primarily clear parasites in a self-destructive mode resulting in thrombocytopenia [25].

Our findings suggest that the secretion of platelets remains active well after parasites are cleared to compensate for platelet loss. This could partly explain the elevation of platelet protein expression at D7 in LMT, however, direct measurement of platelets would be required for confirmation. Our observation that the DAPs are enriched for the creation of C4 and C2 activators, which are proteases produced in activated complement, suggests that the complement is activated to limit

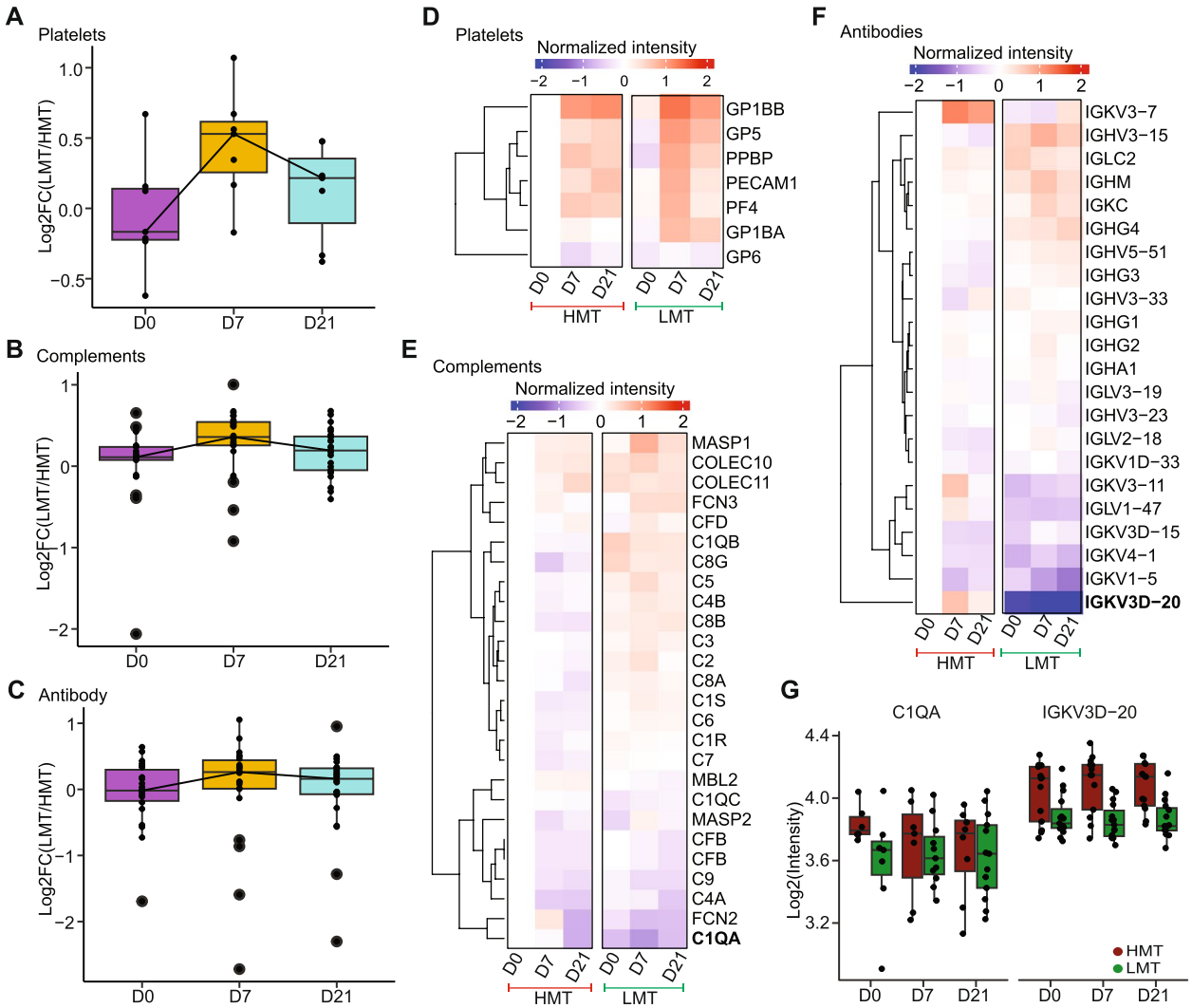

Fig. 5 Platelets, complement factor C1QA, and antibody IGKV3D-20 are strongly associated with malaria exposure. Log2 fold change (LMT/HMT) expression of known (**A**) platelets, (**B**) complements, and (**C**) antibodies proteins for each patient (dots) across the three time-points. Heatmap showing changes in log2 protein intensities (left) and log2FC (right) for (**D**) platelet (normalized intensity to HMT D0), (**E**) complement (normalized intensity to D0), and (**F**) antibody proteins (normalized intensity to HMT D0) across the three time-points. **G** Box plot of log2 run-normalized protein abundance for antibody IGKV3D-20 and complement protein C1QA showing distribution across individual patients (dots)

the progression of malaria infection [reviewed in 15]. These are proteases activated mainly through the classical pathway, which is associated with antigen–antibody binding, and the lectin pathway. The C4 and C2 are downstream components of the complement cascade that split into C3 and C5 convertase, further leading to two main downstream effects, which are inflammation and lysis of infected red blood cells. Further analysis of the intensities of known platelet, complement, and antibody-associated proteins within each site suggest that while there seem to be varying expressions of the complement proteins across the sites, the antibody protein, IGKV3D-20, is clearly more highly expressed in children with more malaria episodes (i.e., HMT group). This could indicate a pre-existing resting immunity prior to detection of the ongoing infection which was absent in the LMT group. These observations support earlier reports in which individuals with more frequent malaria episodes were shown to have a more primed immunity compared to persons with fewer malaria episodes [2, 6, 21]. The complement proteins have also been associated with malaria immune tolerance and protection against malaria in children [26]. Altogether, our findings suggest that there is an association between antibodies and the complement pathway during parasite clearance and the immune tolerance to malaria.

The proteins identified in our study further confirm findings from prior studies on factors associated with malaria immune tolerance. Specifically, we identified the complement cascade and platelet responses as the most enriched immune response pathways. This study also observed that IGKV3D-20 and complement proteins are differentially abundant in HMT compared to LMT areas, suggesting that they are associated with repeated episodes of malaria. It is plausible that repeated infection leads to the accumulation of antimalarial IgM one of which is IGKV3D-20, which in turn promotes activation of the complement cascade thus inhibiting the progression of malaria infection. Our findings suggest that IGKV3D-20 differentiates individuals in HMT and LMT and could be a potential biomarker and/or correlate of naturally acquired immunity.

A limitation of the current study lies in the intrinsic bias of mass spectrometry proteomics to detect highly abundant proteins, which, in plasma, represent platelet proteins, antibodies, and complement proteins. Indeed, the detection of platelet and complement proteins have been reported by similar malaria proteomics studies [26], like this study. Thus, we are limited in our ability to quantify differences in more lowly expressed proteins, including cytokines. Future studies should consider integrating orthogonal assays, such as immunoassays like ELISA or Luminex. Furthermore, using alternative approaches like ELISA or Luminex should be used by future studies to validate the mass spectrometry results presented in this study.

In summary, the plasma proteome of 60 children enrolled from HMT and LMT areas in Ghana was profiled using an unbiased quantitative MS proteomics approach. We identified several biological processes, especially complement cascades and elevated platelets to be associated with increased exposure to malaria. We further identified IGKV3D-20 to be differentially abundant in children from HMT suggesting that it could distinguish individuals with different magnitudes of malaria exposure and, by extension, differing extents of naturally acquired immune tolerance. These proteins could be promising correlates of naturally acquired immunity to malaria and should be further evaluated in larger study cohorts and more mechanistic studies to better understand their functional consequences.

Abbreviations

a.u	arbitrary units
ACN	Acetonitrile
BEH	Ethylene-bridged hybrid inorganic–organic beads
C18	Octyldecylsilane
C1q	complement component 1q
C1QA	Complement component 1q A chain
C2 activators	Complement component c2
C4 activators	Complement component c4
CID	Collision induced dissociation
CSP	Circumsporozoite protein
CV	Coefficient of variation
CyRPA	Cystein-Rich Protective Antigen
Da	Dalton
DAPs	Differentially abundant proteins
DBL3	Duffy binding-like domain 3
DBL5	Duffy binding-like domain 5
DDA	Data dependent acquisition
DAPs	Differentially abundant proteins
DIA	Date independent acquisition
DIA-MS	Data independent acquisition – mass spectrometry
DIA-NN	Data independent acquisition neural networks
EBA140	Erythrocyte binding antigens 140
eV	electron volt
FC	Fold change
FDR	False discovery rate
GLURP-R0	Glutamate rich protein fragment R0
GLURP-R2	Glutamate rich protein fragment R2
GSOA	Gene set overrepresentation analysis
HGNC	HUGO Gene Nomenclature Committee
HMT	High malaria transmission
HPLC-H2O	High performance liquid chromatography water
HPLC–MS	High performance liquid chromatography tandem mass spectrometry
IGKV3D-20	Immunoglobulin kappa variable 3D-20
IgM	Immunogloblin M
IQR	Interquartile range
KHRC	Kintampo health research center
LC	Liquid chromatography
LEKMA	Ledzokuku Krowor municipal assembly
LMT	Low malaria transmission
HMT	High malaria transmission
LOD	Limit of detection
LSA-1	Liver stage specific antigen 1
LysC	Lysine-sensitive aspartokinase 3
MGF	Mascot generic format
MS	Mass spectrometry
MSP1	Merozoite surface protein 1
NMIMR	Noguchi memorial institute for medical research
PASEF	Parallel accumulation serial fragmentation
PCA	Principal component analysis
PPM	Parts per million
TFA	Trifluoroacetic acid
TimsTOF	Trapped ion mobility spectrometry-time of flight
WHO	World Health Organization

Supplementary Information

The online version contains supplementary material available at https://doi.org/10.1186/s12879-025-10495-4.

Supplementary Maerial 1: Figure S1. The correlation between body temperature (reflecting symptomology) and parasitemia (ln(PD/UL)) among study participants at day 0. Figure S2. (A) Hierarchical and k-means clustering of log2 intensities (intensity normalized to HMT D0) to separate proteins into four clusters based on their dynamical regulation over time between LMT and HMT. Log2 intensities of patients from HMT (B) and LMT (C) across different time points.Figure S3. Heatmap summarizing the clustering of proteins across different variables at day 0.

Acknowledgements

We thank all the study participants and their families for their participation and donating blood samples for this study. We also extend our sincere gratitude to the Paul Farmer African Initiative for Research for enabling a collaborative partnership between researchers from institutions in Africa and North America to exchange diverse perspectives that enrich research and drive discovery.

Authors' contributions

Conceptualization, A.M.M., Y.B., and G.A.A.; Investigation, A.M.M, N.K.N., M.B., D.L.S., and A.F.; Formal analysis: C.O.O, M.G, B.J.P., and M.B; Visualization, C.O.O;

Funding acquisition, J.M.F, G.A.A., Y.B., M.B., D.L.S, and N.J.K.; Supervision, J.M.F., D.L.S., G.A.A., N.J.K., M.B., and Y.B., Writing and drafting, A.M.M., and C.O.O.; Critical review and editing, D.L.S., G.A.A., N.J.K., A.F., M.B., and Y.B.

Funding
This work was supported by funds from a World Bank African Centres of Excellence grant (WACCBIP + NCDs: Awandare) and a DELTAS Africa grant (DEL-15–007: Awandare). This research was funded in whole, or in part, by the Wellcome Trust [DEL-15–007] and the UK Foreign, Commonwealth & Development Office, with support from the Developing Excellence in Leadership, Training and Science in Africa (DELTAS Africa) programme. Aisha M. Mohammed was supported by a WACCBIP-World Bank ACE Masters fellowship (WACCBIP + NCDs: Awandare). The study was also supported by a National Institutes of Health (NIH) grant (R01AI152161) awarded to DLS, JMF and NJK and K99AI163868 awarded to MB.

Data availability
All data generated and/or analyzed during this current study is presented in this published work and its supplementary files. The raw mass spectrometry abundance proteomics data files have been deposited to the ProteomeXchange Consortium (http://proteomecentral.proteomexchange.org) via the PRIDE partner repository with the dataset identifiers: Project Name: Plasma proteomics of Ghanian children from high malaria transmission (HMT) and low malaria transmission (LMT) zones Project accession: PXD060218.

Declarations

Ethics approval and consent to participate
The study protocol was reviewed and approved by Noguchi Memorial Institute for Medical Research Institutional Review Board (NMIMR) (Approval number: NMIMR-IRB CPN 008/17–18). Permission to collect samples from the health facilities was granted by the respective hospital managements. All parents or legal guardians of the participants provided written consent prior to recruitment.

Consent for Publication
Not applicable.

Competing interests
The Krogan Laboratory has received research support from Vir Biotechnology, F. Hoffmann-La Roche, and Rezo Therapeutics. Nevan Krogan has a financially compensated consulting agreement with Maze Therapeutics. He is the President and is on the Board of Directors of Rezo Therapeutics, and he is a shareholder in Tenaya Therapeutics, Maze Therapeutics, Rezo Therapeutics, GEn1E Lifesciences, and Interline Therapeutics.

Author details
[1]West African Centre for Cell Biology of Infectious, Pathogens (WACCBIP), College of Basic and Applied Sciences, University of Ghana, Accra, Ghana. [2]Biochemistry, Cell and Molecular Biology, College of Basic and Applied Sciences, University of Ghana, Accra, Ghana. [3]The J. David Gladstone Institute of Data Science and Biotechnology, San Francisco, CA, USA. [4]Quantitative Biosciences Institute, University of California, San Francisco, CA, USA. [5]Department of Bioengineering and Therapeutic Sciences, University of California, San Francisco, CA, USA. [6]Institute for Quantitative and Computational Biosciences (QCBio), University of California, Los Angeles, LA, USA. [7]Department of Microbiology, Immunology, and Molecular Genetics (MIMG), University of California, Los Angeles, LA, USA. [8]Molecular Biology Institute, University of California, Los Angeles, LA, USA. [9]Yemaachi Biotech, Accra, Ghana.

Received: 23 February 2024 Accepted: 13 January 2025
Published online: 03 February 2025

References

1. Gonzales SJ, Reyes RA, Braddom AE, Batugedara G, Bol S, Bunnik EM. Naturally Acquired Humoral Immunity Against Plasmodium falciparum Malaria. Front Immunol. 2020;11:1–15.
2. Hviid L, Barfod L, Fowkes FJI. Trying to remember: Immunological B cell memory to malaria. Trends Parasitol. 2015;31:89–94.
3. World Health Organization. World malaria report 2023. https://www.who.int/teams/global-malaria-programme/reports/world-malaria-report-2023. Accessed 20 Jan 2025.
4. Rathnayake D, Aitken EH, Rogerson SJ. Beyond Binding: The Outcomes of Antibody-Dependent Complement Activation in Human Malaria. Front Immunol. 2021;12:1–11.
5. Bediako Y, Adams R, Reid AJ, Valletta JJ, Ndungu FM, Sodenkamp J, et al. Repeated clinical malaria episodes are associated with modification of the immune system in children. BMC Med. 2019;17:1–14.
6. Crompton PD, Moebius J, Portugal S, Waisberg M, Hart G, Garver LS, et al. Malaria immunity in man and mosquito: Insights into unsolved mysteries of a deadly infectious disease. Annu Rev Immunol. 2014;32:157–87.
7. Griffin JT, Déirdre Hollingsworth T, Reyburn H, Drakeley CJ, Riley EM, Ghani AC. Gradual acquisition of immunity to severe malaria with increasing exposure. Proc R Soc B Biol Sci. 2015;282:1–8.
8. de Jong SE, van Unen V, Manurung MD, Stam KA, Goeman JJ, Jochems SP, et al. Systems analysis and controlled malaria infection in Europeans and Africans elucidate naturally acquired immunity. Nat Immunol. 2021;22:654–65.
9. Proietti C, Krause L, Trieu A, Dodoo D, Gyan B, Koram KA, et al. Immune signature against plasmodium falciparum antigens predicts clinical immunity in distinct malaria endemic communities. Mol Cell Proteomics. 2020;19:101–13.
10. Fowkes FJI, Boeuf P, Beeson JG. Immunity to malaria in an era of declining malaria transmission. Parasitology. 2016;143:139–53.
11. Rono J, Färnert A, Murungi L, Ojal J, Kamuyu G, Guleid F, et al. Multiple clinical episodes of Plasmodium falciparum malaria in a low transmission intensity setting: Exposure versus immunity. BMC Med. 2015;13:1–11.
12. Wiru K, Oppong FB, Gyaase S, Agyei O, Abubakari SW, Amenga-etego S, et al. Annals of GIS Geospatial analysis of malaria mortality in the kintampo health and demographic surveillance area of central Ghana. Ann GIS. 2021;27:139–50.
13. Afrane YA, Zhou G, Githeko AK, Yan G. Clinical malaria case definition and malaria attributable fraction in the highlands of western Kenya. Malar J. 2014;13:1–7.
14. Mensah-Brown HE, Amoako N, Abugri J, Stewart LB, Agongo G, Dickson EK, et al. Analysis of erythrocyte invasion mechanisms of plasmodium falciparum clinical isolates across 3 malaria-endemic areas in Ghana. J Infect Dis. 2015;212:1288–97.
15. Fossati A, Richards AL, Chen KH, Jaganath D, Cattamanchi A, Ernst JD, Swaney DL. Toward comprehensive plasma proteomics by orthogonal protease digestion. J Proteome Res. 2021;20(8):4031–40.
16. Demichev V, Szyrwiel L, Yu F, Teo GC, Rosenberger G, Niewienda A, Ludwig D, Decker J, Kaspar-Schoenefeld S, Lilley KS, Mülleder M, Nesvizhskii AI, Ralser M. dia-PASEF data analysis using FragPipe and DIA-NN for deep proteomics of low sample amounts. Nat Comm. 2022;13:1–8.
17. Bouhaddou M, Reuschl A-K, Polacco BJ, Thorne LG, Ummadi MR, Ye C, et al. SARS-CoV-2 variants evolve convergent strategies to remodel the host response. Cell. 2023;186:4597-4614.e26.
18. Ghana Demorgraphic and Health Survey Report, Ghana. 2022. https://statsghana.gov.gh/gdhs/page/fes%20materials.html. Retrieved on 09th May, 2024.
19. Shu T, Ning W, Wu D, Xu J, Han Q, Huang M, et al. Plasma Proteomics Identify Biomarkers and Pathogenesis of COVID-19. Immunity. 2020;53:1108-1122.e5.
20. Reuterswärd P, Bergström S, Orikiiriza J, Lindquist E, Bergström S, Andersson Svahn H, Nilsson P. Levels of human proteins in plasma associated with acute paediatric malaria. Malar J. 2018;17:1–19.
21. Kurtovic L, Behet MC, Feng G, Reiling L, Chelimo K, Dent AE, et al. Human antibodies activate complement against Plasmodium falciparum sporozoites, and are associated with protection against malaria in children. BMC Med. 2018;16:1–17.
22. Nyakoe NK, Taylor RP, Makumi JN, Waitumbi JN. Complement consumption in children with Plasmodium falciparum malaria. Malar J. 2009;8:3–10.
23. Korir JC, Nyakoe NK, Awinda G, Waitumbi JN. Complement activation by merozoite antigens of Plasmodium falciparum. PLoS ONE. 2014;9(8):e105093.

24. Kho S, Barber BE, Johar E, Andries B, Poespoprodjo JR, Kenangalem E, McMorran BJ. Platelets kill circulating parasites of all major Plasmodium species in human malaria. Blood J Am Soc Hematol. 2018;132(12):1332–44.
25. McMorran BJ. Immune role of platelets in malaria. ISBT Sci Ser. 2019;14:67–76.
26. Kurtovic L, Boyle MJ, Opi DH, Kennedy AT, Tham WH, Reiling L, et al. Complement in malaria immunity and vaccines. Immunol Rev. 2020;293:38–56.

Publisher's Note